Robust Modeling and Linearization of MIMO RF Power Amplifiers for 4G and 5G Applications

Imene ZEMZEMI, Souhir LEJNEF
Dept. of Physics, Faculty of Sciences of Tunis,
University of Tunis El Manar,
Tunis, Tunisia

Noureddine BOULEJFEN
Research Center for Microelectronics and Nanotechnology,
Technopole Sousse,
Sousse, Tunisia

M.Fadhel GHANNOUCHI
iRadio Laboratory, Electrical Engineering Department, Schulich Engineering School,
University of Calgary 2500 University Drive NW, Calgary, Alberta 2TN 1N4, Canada

Abstract—**In this paper, a novel set of orthogonal crossover polynomials for the baseband modelling and linearization of MIMO RF Pas is presented. The proposed solution is applicable to WCDMA and LTE applications. The new modelling approach has considerably reduced the numerical instability problem associated with the conventional polynomial model identification. In order to validate the efficiency and the robustness of the proposed solution, a 2x2 MIMO LDMOS RF power amplifier has been measured modelled and linearized. A comparison with the conventional polynomial MIMO models showed clearly the superiority of the proposed solution in a fixed-point calculation environment such as DSP and FPGA boards.**

Keywords—*MIMO transmitter; RF power amplifiers; orthogonal polynomials; nonlinear transmitters; digital predistortion*

I. INTRODUCTION

Power amplifiers (PAs) are the major source of nonlinearity in communication system that causes spectral regrowth as well as in-band distortion. Accurate modeling of the RF PAs is required which increases the problem size and reduces the numerical stability of the model identification procedure. This problem is more pronounced in multiple input systems. Multiple-input multiple-output (MIMO) transceivers allow high service quality and increase the capacity range of wireless transmission requiring very high-speed data transfer [1]–[3]. In fact, the capacity of MIMO transceivers M times the capacity of a single-input-single-output (SISO) equivalent system. Volterra series were developed in [4]–[7] and were intensively used in modelling power amplifiers and DPD. However, the Volterra series involves a great number of coefficients, which increases the complexity of the problem in the case of MIMO systems.

In the literature, several attempts reduce the number of coefficients for PA models. In [8] a dynamic deviation reduction model has been suggested for modelling single input PAs. In [9]–[13], reduced polynomial models have been proposed for modelling MIMO PAs. Saffar et al. [14], addressed the joint mitigation of I/Q modulator impairment and PA nonlinearity in MIMO transmitters through an optimized memory polynomial model. However, all these published

models suffer from the increasing numerical instability as the problem size increases. This generally happens when a high nonlinearity order, a high memory depth, or a big number of inputs were considered.

Radio frequency (RF) PAs presents a challenge to the transceiver designers. In fact, designers need to boost two contradictory parameters of the PA such as power efficiency and linearity. Several linearization techniques are proposed in the literature to improve PA's linearity. Due to its simplicity and efficiency, the digital pre-distortion (DPD) is considered as the most popular linearization technique. Hence, the DPD approach has been intensively used to compensate for the transmitter nonlinearities as in [15]–[17]. However, the DPD technique requires an accurate modelling of the PA. In fact, high polynomial order leads generally to an accurate model with high complexity. This generally increases the numerical instability and vulnerability of the model identification procedure [18], [19]. Therefore, a tradeoff is always required between the model accuracy and complexity. A good metric for measuring the model accuracy is the time domain normalized mean squared error (NMSE) while the DPD performance can be measured using the frequency domain adjacent channel power ratio (ACPR) of the compensated system [20], [21]. However, the model identification procedure is based on the inversion of an observation matrix that has to be well conditioned in order to avoid numerical instability. The condition number is a metric to test the conditioning of this matrix by measuring the linear dependence of its columns [18], and is generally related to the distribution of the input signal envelope, as well as the dimensionality of the problem. In MIMO PAs, the problem size increases drastically with the number of input signals, making the instability issue more pronounced. This is mainly due to the high correlation that can exist between the input data resulting in ill-conditioned observation matrix with a high condition number. In this work, the numerical instability of the model identification procedure is addressed through the development of a complex multi-input orthogonal polynomial model.

The organization of the paper is as follows. In Section. 2, we introduce the reference crossover conventional polynomials

for modelling the MIMO PAs. In Section 3, we present the derived novel robust orthogonal polynomial model. The experimental validation and performance assessment of the proposed model is given in Section 4. Finally, the conclusion is drawn in Section 5.

II. MODELLING MIMO SYSTEMS USING CONVENTIONAL POLYNOMIALS

In this section, the crossover polynomial model [13] is detailed, and its limitations are discussed for a 2×2 MIMO PA case. The conventional polynomial model is a base band model that has been developed to characterizing nonlinear radio frequency power amplifiers with and without memory effects. The closed form expression that relates the input and output complex envelope signals of the PA is given in [13] such that

$$y_i(n) = \sum_{j=1}^{2} \sum_{q=0}^{Q} \sum_{p=0}^{P} \sum_{k=0}^{K} h_{k,p,q}^{j,i} \, x_j(n-p) \left| x_j(n-p-q) \right|^{2k} \quad (1)$$

where x_j and y_i are the complex envelope input and output signals respectively and $h_{k,p,q}^{i,j}$ are the model coefficients with $i, j \in \{1,2\}$. K is the model nonlinearity and P and Q are the memory depths.

Equations (1) can be expressed in a matrix form such that

$$\begin{bmatrix} \vec{y_1} & \vec{y_2} \end{bmatrix} = \begin{bmatrix} \Phi_{\vec{x_1}} & \Phi_{\vec{x_2}} \end{bmatrix} \begin{bmatrix} \overrightarrow{H^{1,1}} & \overrightarrow{H^{1,2}} \\ \overrightarrow{H^{2,1}} & \overrightarrow{H^{2,2}} \end{bmatrix} \quad (2)$$

For a two-input single output memory less polynomial conventional model, the above expression becomes.

$$\vec{y_1} = \begin{bmatrix} \Phi_{\vec{x_1}} & \Phi_{\vec{x_2}} \end{bmatrix} \begin{bmatrix} \overrightarrow{H^{1,1}} \\ \overrightarrow{H^{2,1}} \end{bmatrix} \quad (3)$$

where $\Phi_{\vec{x_1}}$ and $\Phi_{\vec{x_2}}$ are the data matrices defined for inputs $\{x_1, x_2\}$ and $\overrightarrow{H^{1,1}}$, $\overrightarrow{H^{2,1}}$ are the vectors of complex-valued model coefficients between the inputs and the output $\vec{y_1}$ such that

$$\vec{y_1} = \begin{bmatrix} y_1(1), y_1(2), y_1(3), ..., y_1(S) \end{bmatrix} \quad (4)$$

where S is the number of input samples.

$$H = \begin{bmatrix} \overrightarrow{H^{1,1}} \\ \overrightarrow{H^{2,1}} \end{bmatrix} = \begin{bmatrix} h_0^{1,1}, h_1^{1,1}, ..., h_k^{1,1}, h_0^{2,1}, h_1^{2,1}, ..., h_k^{2,1} \end{bmatrix}^T \quad (5)$$

is a vector of the model coefficients.

$\Phi = \begin{bmatrix} \Phi_{\vec{x_1}} & \Phi_{\vec{x_2}} \end{bmatrix}$ is a matrix such that:

$$\Phi_{\vec{x_j}} = \begin{bmatrix} \phi_0(x_j(1)) & \cdots & \phi_K(x_j(1)) \\ \vdots & \ddots & \vdots \\ \phi_0(x_j(S)) & \cdots & \phi_K(x_j(S)) \end{bmatrix} \quad (6)$$

with $\phi_K(x)$ is given by $\phi_K(x) = x|x|^{2K}$.

The least-squares estimate (LSE) of H for MIMO conventional models can be obtained using the Moore-Penrose pseudo inversion such that

$$\vec{H}_{\text{LS}} = (\Phi^H \Phi)^{-1} \Phi^H \vec{y_1} \quad (7)$$

where $[\cdot]^H$ denotes the Hermitian transpose.

The inversion of the observation matrix $M = \begin{bmatrix} \Phi^H \Phi \end{bmatrix}$ is often imperfectly conditioned. Thus, the inversion of such matrix will undergo numerical errors. This problem is more pronounced and leads to erroneous results when the finite precision calculation is used. Define the condition number of a matrix M as:

$$\rho(M) = \left(\left| \frac{\lambda_{\max}(M)}{\lambda_{\min}(M)} \right| \right) \quad (8)$$

where $\lambda_{\max}$ and $\lambda_{\min}$ are the maximum and minimum singular values of M.

In order to estimate the condition number ρ of the observation matrix $\begin{bmatrix} \Phi^H \Phi \end{bmatrix}$, two independent sets $\{x_1, x_2\}$ of 184,239 data samples with normalized Gaussian distribution are used.
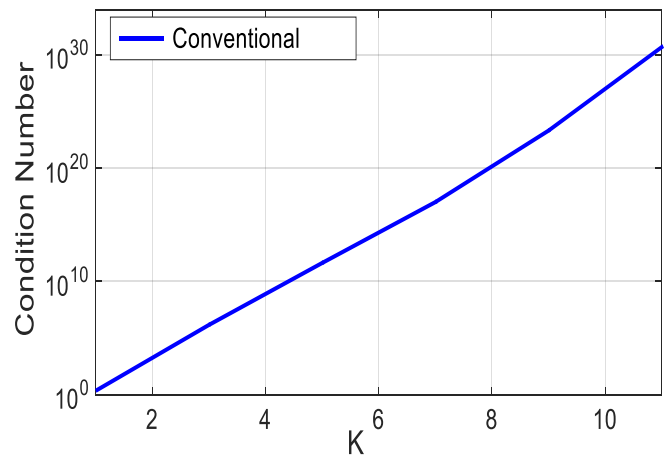

Fig. 1. The condition number of $\begin{bmatrix} \Phi^H \Phi \end{bmatrix}$ as a function of K.

Fig. 1 shows clearly that the condition number ρ increases exponentially as a function of the model nonlinearity order. This implies that, in practice, the model can be unstable. Therefore, reduction of the condition number is highly required to ensure the numerical stability of the model coefficient identification procedure. This can be achieved by substituting the set of conventional basis functions $\phi_K(x)$ with an orthogonal set $\psi_K(x)$ leading to an observation matrix with lower ρ.

III. ORTHOGONAL POLYNOMIALS BASED MODEL FOR MIMO RF POWER AMPLIFIERS

In this section, we propose a new set of orthogonal polynomial basis functions for modelling PAs excited with two independent signals. To adhere to the statistics of the widely used communication signals such as WCDMA and LTE, Gaussian distributions have been considered for the complex envelops of the RF inputs. The proposed solution is expected to reduce the condition number of the observation matrix and hence ensure the numerical stability of the model identification procedure.

Considering the memory less case and in an attempt to alleviate the numerical instability problem associated with the inversion of the observation matrix in (6) let's consider

$$y_i(n) = \sum_{j=1}^{2} \sum_{k=0}^{K} b_k^{j,i} \sum_{l=0}^{k} u_{j,lk} x_j(n) \left| x_j(n) \right|^{2k} \qquad (9)$$

where x_j and y_i are the complex envelope input and output signals respectively and $b_k^{i,j}$ are the model coefficients, $u_{j,lk}$ are the coefficients of the orthogonal model, P and Q are the memory depths, K is the model nonlinearity, with $i, j \in \{1, 2\}$.

The new data matrix is given by

$$\Psi = \begin{bmatrix} \Psi_{\overrightarrow{x_1}} & \Psi_{\overrightarrow{x_2}} \end{bmatrix} = \begin{bmatrix} \Phi_{\overrightarrow{x_1}} & \Phi_{\overrightarrow{x_2}} \end{bmatrix} U \qquad (10)$$

with U is a $(2k+2) \times (2k+2)$ matrix.

We consider the following requirements for the orthogonality of the suggested basis functions: $\Psi_k(x)$ and $\Psi_\ell(x)$ to be orthogonal, the following condition has to be satisfied:

$$\begin{cases} E\left[\Psi_k^*(x)\ \Psi_\ell(x) \right] = 0 & if\ k \neq \ell \\ E\left[\Psi_k^*(x)\ \Psi_\ell(x) \right] = 1 & if\ k = \ell \end{cases} \qquad (11)$$

Where, E[.] denotes statistical expectation, and (*) stands for complex conjugation. Therefore, finding the appropriate orthogonal polynomial basis functions returns to finding the U matrix such that

$$E\left[\Psi^H \Psi \right] = U^H E\left[\Phi^H \Phi \right] U = S U^H M\ U \qquad (12)$$

is diagonal, with $M = E\left[\Phi^H \Phi \right]$ is a $(2K+2) \times (2K+2)$ matrix. The resolution of the problem returns to find the elements of the matrix U such that $U^H M\ U = I_d$.

To find the U matrix elements for the proposed 2×2 MIMO model consider x_1 and x_2 two independent complexes Gaussian input signals with zero means and variances σ_{x1} and σ_{x2} respectively. The $E\left[\Phi^H \Phi \right]$ matrix can then be given by

$$E\left[\Phi^H\ \Phi \right] = \begin{bmatrix} R_1 & 0_{k+1} \\ 0_{k+1} & R_2 \end{bmatrix} \qquad (13)$$

where 0_{k+1} is a $(k+1) \times (k+1)$ sub matrix with zero elements. R_1 and R_2 are two $(k+1) \times (k+1)$ symmetric sub-matrices such that for $i = \{1, 2\}$ we have

$$R_i = E \begin{bmatrix} |x_i|^2 & \cdots & |x_i|^{2k+2} \\ \vdots & \ddots & \vdots \\ |x_i|^{2k+2} & \cdots & |x_i|^{4k+2} \end{bmatrix} \qquad (14)$$

To construct the required set of basis functions the U matrix is proposed to be a $(2k+2) \times (2k+2)$ matrix such that

$$U = \begin{bmatrix} U_1 & 0_{k+1} \\ 0_{k+1} & U_2 \end{bmatrix} \qquad (15)$$

Where, U_1 and U_2 are $(k+1) \times (k+1)$ upper triangular sub-matrices such that

$$U_i = \begin{bmatrix} u_{i,00} & \cdots & u_{i,0k} \\ 0 & \ddots & \vdots \\ 0 & 0 & u_{i,lk} \end{bmatrix} \qquad (16)$$

and 0_{k+1} is a null $(k+1) \times (k+1)$ sub matrix. For the proposed 2×2 MIMO model with two independent inputs x_1 and x_2 with zero mean and σ_{x_i} variances. The $u_{i,lk}$ elements of the matrix U_i can be given by [19].

$$U_i = \begin{cases} \dfrac{(-1)^{k-\ell}}{\sigma_{x_i}^{2k+1}} \dfrac{\sqrt{k+1}}{(\ell+1)!} \begin{pmatrix} \ell \\ k \end{pmatrix} & \ell \leq k \\ 0 & \ell > k \end{cases} \qquad (17)$$

with $i = \{1, 2\}$ refers to the inputs of the PA.

A. N×N MIMO Orthogonal Crossover Model

The suggested Crossover orthogonal model can be extended to *N×N* MIMO transmitters such that:

$$\begin{bmatrix} \vec{y_1} & \vec{y_2} \cdots \vec{y_N} \end{bmatrix} = \begin{bmatrix} \Phi_{\vec{x_1}} & \Phi_{\vec{x_2}} \ldots \Phi_{\vec{x_N}} \end{bmatrix} \begin{bmatrix} \overrightarrow{H^{1,1}} & \cdots & \overrightarrow{H^{N,1}} \\ \vdots & \ddots & \vdots \\ \overrightarrow{H^{1,N}} & \cdots & \overrightarrow{H^{N,N}} \end{bmatrix} \quad (20)$$

with *N* is the number of inputs and outputs of the MIMO transmitter.

For MISO transmitters with *N* inputs and a single output, expression (9) leads to the following matrix form:

$$\vec{y_1} = \begin{bmatrix} \Phi_{\vec{x_1}} & \Phi_{\vec{x_2}} \ldots \Phi_{\vec{x_N}} \end{bmatrix} \begin{bmatrix} \overrightarrow{H^{1,1}} \\ \vdots \\ \overrightarrow{H^{1,N}} \end{bmatrix} \quad (21)$$

In order to convert the observation matrix to a diagonal one that ensures the numerical stability of the model identification procedure, the F matrix is substituted with a Y matrix such that

$$\Psi = \begin{bmatrix} \Psi_{\vec{x_1}} & \Psi_{\vec{x_2}} \ldots \Psi_{\vec{x_N}} \end{bmatrix} = \begin{bmatrix} \Phi_{\vec{x_1}} & \Phi_{\vec{x_2}} \ldots \Phi_{\vec{x_N}} \end{bmatrix} U \quad (22)$$

with U is an (Nk+N)×(Nk+N) orthogonal matrix. U is composed of sub matrices U$_i$ placed in the diagonal line with $i=\{1,2,\ldots,N\}$,such that:

$$U = \begin{bmatrix} U_1 & 0_{k+1} & \cdots\cdots & 0_{k+1} \\ 0_{k+1} & U_2 & & \vdots \\ \vdots & & \ddots & 0_{k+1} \\ 0_{k+1} & \cdots & 0_{k+1} & U_N \end{bmatrix} \quad (23)$$

B. Numerical Validation

In this paper, we proposed a closed-form expression for orthogonal polynomials to model MIMO Pas excited by RF signals with Gaussian complex envelops such as WCDMA and LTE signals. To demonstrate the efficiency of the proposed set of basis functions in reducing the risk of numerical instability, the condition number of the resulting observation matrix has been calculated. To do so 184,239 independent realizations of a four-channel WCDMA1001 and a four-channel WCDA1111 have been generated as input signals x_1 and x_2 respectively and used to calculate the $\Phi^H\Phi$ and $\Psi^H\Psi$ observation matrices for different non-linearity orders *K*. The '1' refers to an ON channel while the '0' refers to an OFF channel. Fig. 2 shows the condition number for the memory less 2×2 MIMO.

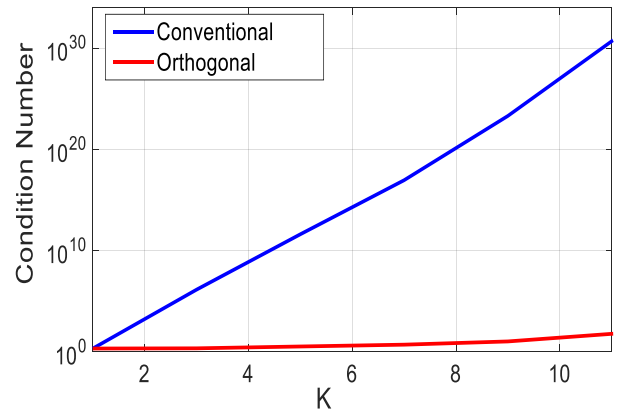Fig. 2. The condition number of $\Phi^H\Phi$ and $\Psi^H\Psi$ for the 2×2 MIMO case.

Fig. 2 shows clearly that for the conventional model the condition number grows exponentially with the non-linearity order *K* to reach 10^{30} for *K*=11. However, for the proposed orthogonal model, the condition number increases at a much lower rate without exceeding 100 for the same range of *K*.

Hitherto, the above-described numerical simulations have proven the remarkable performance of the proposed orthogonal polynomial basis functions for crossover 2×2 MIMO models. However, an experimental validation is required to verify the impact of the numerical stability on the model accuracy.

IV. EXPERIMENTAL VALIDATION

The performances of the proposed set of orthogonal basis functions have been evaluated by modelling and linearizing a 2x2 RF power amplifier. To do so the experimental setup shown in Fig. 3 has been developed. We generated two signals using two vector signal generators (VSG) ESG1 and ESG2 of type E4438C in order to excite the MIMO transmitter. The latter is equivalent to two drivers followed by two class-AB RF PAs and two attenuators. Two couplers have been used to introduce a non-linear cross talk as shown in the figure. A vector signal analyzer (VSA) of type E4440A is then used to collect and analyze one of the two attenuators' outputs through the RF switch.
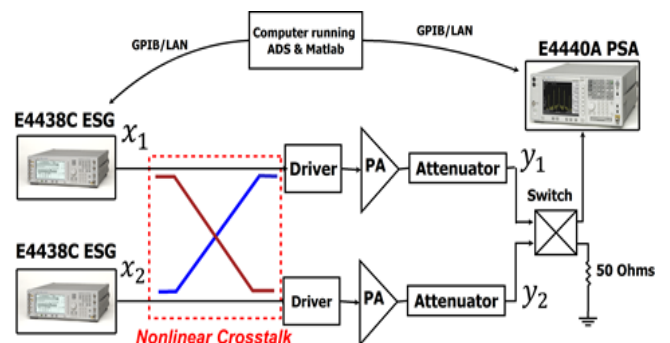

Fig. 3. Block Diagram of a MIMO PA measurement setup.

The measurement is performed by connecting the sources via a (GPIB) bus. The I/Q components of the two multi-carrier wideband code division multiple access (WCDMA) signals (WCDMA1001 and WCDMA1111) are generated using Matlab then downloaded to the source with an average power equal to 9 dBm and a bandwidth of 20 MHz. The output signal is down-converted, sampled and digitized at a sampling frequency of (*fs*= 92.16MHz) for a time window of 2ms leading to a data set of 184,239 samples. The non-linear crosstalk is set to −20 dB

C. Key Performance Metrics

To evaluate the accuracy of the proposed MIMO model in predicting the transmitter output the time domain normalized mean square error (NMSE) has been used. The NMSE [20], [21] is expressed in the logarithmic scale as shown in the following equation:

$$NMSE_{dB} = 10\log_{10}\left[\frac{\sum_{n=1}^{N}\left|y_i(nT_S) - y_m(nT_S)\right|^2}{\sum_{n=1}^{N}\left|y_i(nT_S)\right|^2}\right] \quad (24)$$

where $y_i(nT_S)$ and $y_m(nT_S)$ are respectively the complex envelopes of the measured and modelled output signals. In the other hand, a frequency domain metric such as the adjacent channel power ration (ACPR) can be used to evaluate the spectral regrowth in the output spectrum as well as the performances of the proposed model based digital predistorter. The ACPR defined as follows [20], [21]:

$$ACPR_{dB} = \frac{\int_{Adj.ch}\left|Y(f)\right|^2 df}{\int_{main.ch}\left|Y(f)\right|^2 df} \quad (25)$$

The adjacent channel power ration (ACPR) is measured for the adjacent channels below and above the main carrier in dBc.

D. Forward Model Experimental Results

The importance of a low condition number resides in the fact that the PA model is generally used in the PAs linearization operation. The linearization algorithm runs on a fixed-point processor like DSP or FPGA with a limited number of bits. In fact, the fixed-point processors are efficient with low computation time, cost and power consumption. However, during the modelling process, the model is generally simulated with a floating-point processor.

The nonlinearity order is set to 11 and the memory depths *P* and *Q* are set to 2 and 3 respectively. Under these conditions, three different calculation environments have been considered.

- Scenario 1: floating point calculation.

- Scenario 2: fixed point calculation with a fraction length of 32 bits.

- Scenario 3: fixed point calculation with a fraction length of 24bits.

As a first test, the coefficients of the conventional and the proposed orthogonal models for the PA under test have been identified in a floating calculation environment. The models' outputs are then compared to the measured PA output and the NMSE have been calculated. Fig. 4(a) shows the NMSE of the two models. The figure reveals that the two models exhibit a comparable accuracy with a pretty similar NMSEs that reached -47.5dB for *K* = 10. However, the NMSE of the conventional model bounced back to -42dB for *K* = 11 while the one of the proposed models continued its fall to -48.53dB.
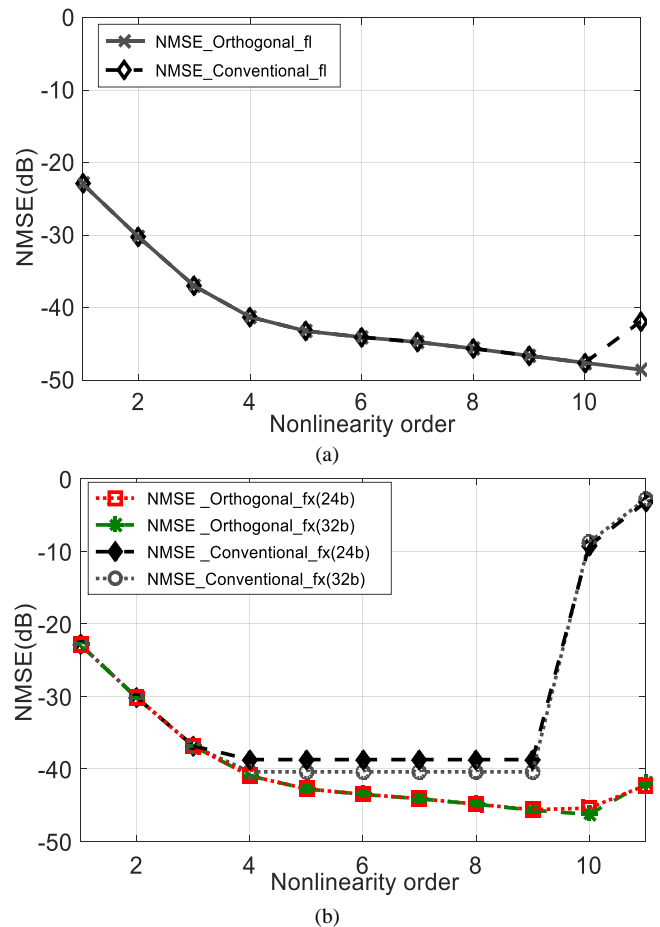

Fig. 4. Measurement of the NMSE of scenario 1(a), scenario 2 and scenario 3(b).

In a second test, the same procedure has been repeated using a 64 bits fixed-point processor with fractional lengths of 32 bits and 24 bits. Fig. 4(b) shows The NMSEs for the two models and for the two fraction lengths. The figure demonstrates clearly that the performance of the conventional model deteriorates for the two cases leading to NMSEs diverging to near -3dB for K = 11. However, the proposed orthogonal model maintained its accuracy with NMSEs below -40dB for the whole range of *K*.

E. Digital Pre-Distorter Experimental Results

Once the coefficients of the model are identified, the PA output can be predicted under different excitation signals. However, in an attempt to linearize the PA and improve its efficiency-linearity compromise, a reverse model can be developed and a digital predistorter (DPD) can be obtained using the indirect learning architecture (ILA). As shown in Fig. 5, the ILA consists of identifying and updating the DPD coefficients using the LS algorithm while exchanging the PA inputs and outputs. The resulting DPD can then linearize the PA and improve the quality of its output spectrum. To validate the effectiveness of the proposed orthogonal model in the linearization of MIMO PAs, a nonlinearity order of 11 and memory depths P and Q of 2 and 3, respectively were considered. The DPD is then developed and applied using the three different scenarios of calculation environment.
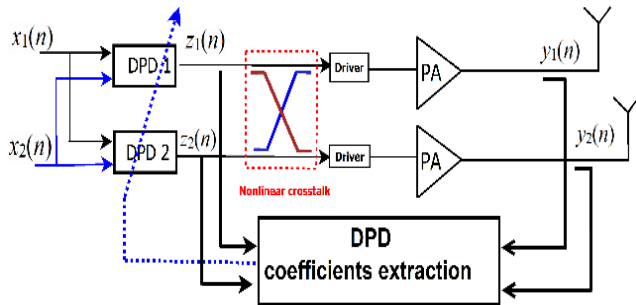
Tables I, II and III show the adjacent channel power ratios (ACPR) of the 2x2 MIMO PA outputs with and without DPD. The table revealed the high values (above -28dBc) of the ACPR for the different scenarios when the DPD is turned OFF. Under the floating-point environment calculation, the conventional and the proposed orthogonal model based DPDs performed pretty well with an ACPR below -42dBc for the two PA outputs. In addition, the results revealed a better performance of the orthogonal model based DPD with an ACPR as low as -49dBc.

Under the fixed-point calculation environment, the performance of the conventional model-based DPD deteriorates significantly, leading to an ACPR exceeding -19dBc. However, the orthogonal model based DPD maintained its good performance with an ACPR below -41dBc for the two PA outputs and for the two fraction lengths of 24 and 32 bits

Fig. 5.   Block Diagram of a MIMO PAs + DPD measurement setup.

TABLE I.   MEASURED ACPR IN DBC FOR THE FIRST SCENARIO

Signal	WCDMA1001		WCDMA1111	
	L	R	L	R
Without DPD	-33.42	-32.76	-34.42	-34.61
With DPD (conventional model)	-42.25	-42.60	-43.56	-43.81
With DPD (orthogonal model)	-49.16	-49.31	-50.21	-50.30

TABLE II.   MEASURED ACPR IN DBC FOR THE SECOND SCENARIO
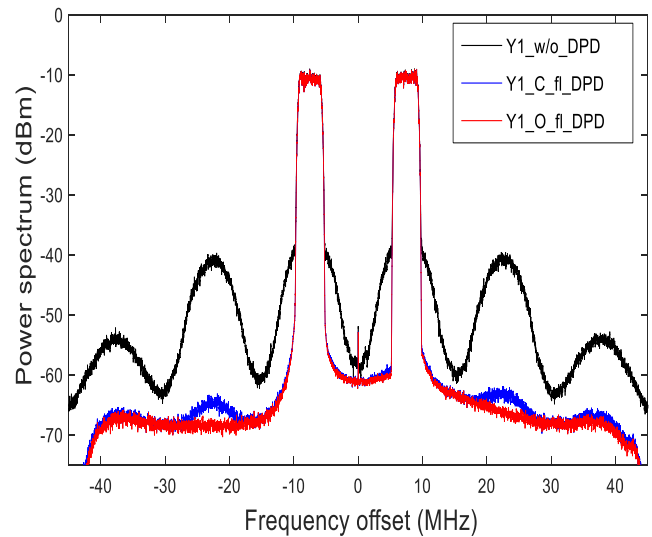
Signal	WCDMA1001		WCDMA1111	
	L	R	L	R
Without DPD	-28.52	-28.92	-28.76	-28.33
With DPD (conventional model)	-20.29	-20.32	-20.34	-20.79
With DPD (orthogonal model)	-42.97	-43.1	-43.52	-43.86

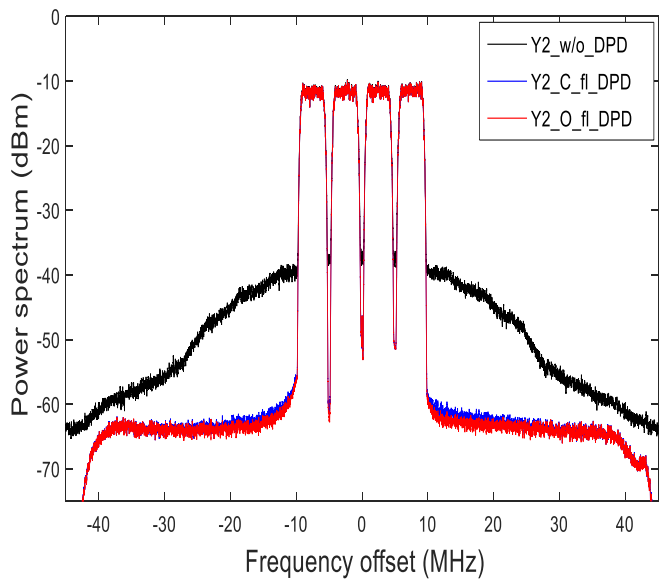TABLE III.   MEASURED ACPR IN DBC FOR THE THIRD SCENARIO

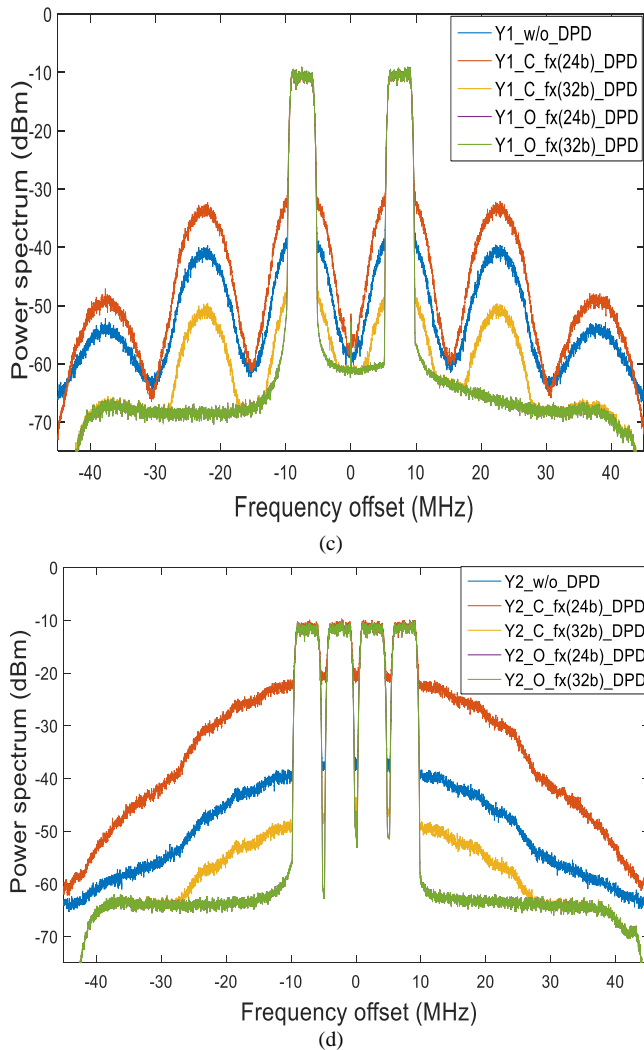| Signal	WCDMA1001		WCDMA1111	
	L	R	L	R
Without DPD	-27.58	-27.92	-27.77	-27.91
With DPD (conventional model)	-18.37	-18.41	-19.21	-19.34
With DPD (orthogonal model)	-41.87	-41.62	-42.64	-42.32

(a)

(b)

Fig. 6.   Frequency domain performance for two channels for 2×2 MIMO transmitter (a) and (b) outputs of DPD for scenario 1, (c) and (d) outputs of DPD for scenario 2 and 3.

In Fig. 6 the power spectral densities of the PA outputs has been plotted for the different scenarios where Yi_w/o_DPD are the measured PA outputs when the DPD is turned OFF (Black); Yi_C_fl_DPD are the predicted PA outputs when the conventional model based DPD is applied using a floating point calculation environment (Blue); Yi_O_fl_DPD are the predicted PA outputs when the orthogonal model based DPD is applied using a floating point calculation environment (Red); Yi_C_fx(24b)_DPD are the predicted PA outputs when the conventional model based DPD is applied using a fixed point calculation environment with a fraction length of 24 bits (Orange); Yi_C_fx(32b)_DPD are the predicted PA outputs when the conventional model based DPD is applied using a fixed point calculation environment with a fraction length of 32 bits (Yellow); Yi_O_fx(24b)_DPD are the predicted PA outputs when the orthogonal model based DPD is applied using a fixed point calculation environment with a fraction length of 24 bits (Violet); Yi_O_fx(32b)_DPD are the predicted PA outputs when the orthogonal model based DPD is applied using

a fixed point calculation environment with a fraction length of 32 bits (Green), with $i = \{1,2\}$ denotes the number of outputs.

Fig. 6 shows the power spectral densities of the predicted PA outputs for the different scenarios. The measured outputs of the nonlinearity PA, shown in Fig. 6(a)-(b), confirm the spectrum regrowth caused by the PA nonlinearity. In the same time, the figures reveal quite similar and perfect PA linearization when using a floating-point processor (scenario 1) regardless of the DPD model. However, Fig. 6(c)-(d) shows the spectra of the same signals in the cases of scenario 2 and 3. The figures reveal that when using a fixed-point processor, the conventional model-based DPD loses completely its performance and fail to linearize the PA. However, the proposed orthogonal model based DPD maintains its good performances and succeeds to linearize the PA for the 32 bits and 24 bits fraction lengths.

V.   CONCLUSION

In this paper, we proposed closed-form expressions for orthogonal polynomials for MIMO PA modelling under RF signals with Gaussian complex envelopes. The numerical and experimental validations have confirmed the robustness and stability of the proposed model identified in fixed-point calculation environments. The proposed orthogonal model based DPD outperformed the conventional model-based DPD in terms of adjacent channel emission reduction in the presence of a nonlinear coupling in the MIMO PA. Due to its simplicity and closed-form expression, the proposed model can be tuned to fit special cases such as massive MIMO PAs where only the coupling between adjacent inputs needs to be considered.

REFERENCES

[1]   J. Gozalvez, "Samsung Electronics Sets 5G Speed Record at 7.5 Gb/s [Mobile Radio],"*IEEE Vehicular Technology Magazine*,vol.10,no.1, p.12–16, 2015

[2]   G.J.Foschini and M. J. Gans, "On limits of wireless communications in a fading environment when using multiple antennas," *Wireless Pers. Commun.*, vol. 6, no. 3, pp. 311–335, Mar. 1998.

[3]   N. Doose, P.A. Hoeher, "Massive MIMO Ultra-Wideband Communications Using Multi-Mode Antennas,"*In 10th International ITG Conference on Systems Communications and Coding (SCC)*, Hambourg (Allemagne),* pp. 1–6, 2015.

[4]   L. Chua and C.-Y. Ng, "Frequency domain analysis of nonlinear systems: general theory*," IEE Journal on Electronic Circuits and Systems*, vol. 3, no. 4,pp. 165–185, Jul. 1979.

[5]   A. K. Swain and S. A. Billings, "Generalized frequency response function matrix for MIMO non-linear systems," *Int. J.Control*, vol. 74, no. 8, pp. 829–844, 2001.

[6]   L. M. Li and S. A. Billings, "Generalized frequency response functions and output response synthesis for MIMO non-linear systems," *Int.J. Control*, vol. 79, no. 1, pp. 53–62, 2006.

[7]   Z. K. Peng, Z. Q. Lang, and S. A. Billings, "Non-linear output frequency response functions for multi-input non-linear volterra systems,"*Int. J. Control*, vol. 80, no. 6, pp. 843–855, 2007.

[8]   A. Zhu, J. Pedro, and T. Brazil, "Dynamic deviation reduction-based Volterra behavioral modeling of RF power amplifiers," *IEEE Trans. Microw. Theory Tech.*, vol. 54, no. 12, pp. 4323–4332, Dec. 2006.

[9]   D. Saffar, N. Boulejfen, F.M. Ghannouchi, et al,"Compensation of I/Q Impairments and Nonlinear Distortion in MIMO Wireless Transmitters,"*In 11th IEEE International New Circuits and Systems Conference (NEWCAS), Paris (France)*, pp. 1–4, 2013.

[10] S. A. Bassam, M. Helaoui, F.M. Ghannouchi, "2-D digital predistortion (2-D-DPD) architecture for concurrent dual-band transmitters*," IEEE*

Transactions on Microwave Theory and Techniques, vol. 59, no. 10, pp. 2547–2553, 2011.

[11] S. A. Bassam, M. Helaoui, F.M. Ghannouchi, "Crossover digital predistorter for the compensation of crosstalk and nonlinearity in MIMO transmitter;"*IEEE Transactions on Microwave Theory and Techniques*, vol. 57, no. 5, pp. 1119–1128, 2009.

[12] E. Zenteno, S. Amin, M. Isaksson, D. Ronnow and P. Handel, "Combating the dimensionality of nonlinear MIMO amplifier predistortion by basis pursuit,"*IEEE EuMC* 2014, Rome, Italy, pp. 822-826, 6-9 Oct. 2014.

[13] S Amin, P. N. Landin, P. Handel, D. Ronnow, "Behavioral Modeling and Linearization of Crosstalk and Memory Effects in RF MIMO Transmitters,"*IEEE Transactions on Microwave Theory and Techniques,* vol. 62, no. 4, pp. 810–823, 2014.

[14] D. Saffar, N. Boulejfen, F.M. Ghannouchi et al, "Behavioral modeling of MIMO nonlinear systems with multivariable polynomials," *IEEE Transactions on Microwave Theory and Techniques*, vol. 59, no. 11,pp. 2994–3003, 2011.

[15] M. Younes, F.M. Ghannouchi,"Behavioral Modeling of Concurrent Dual-band Transmitters based on Radial-Pruned Volterra Model,"*IEEE Communications Letters*, vol. 19, no. 5, pp.751–754, 2015.

[16] F. Zhu, L. Anttila, M. Abdelaziz, et al., "Frequency-Selective Digital Predistortion for Unwanted Emission Reduction,"*IEEE Transactions on Communications,* vol. 63, no. 1, pp.254–267, 2015.

[17] A. Molina, K. Rajamani, K. Azadet, "Digital Predistortion Using Lookup Tables With Linear Interpolation and Extrapolation: Direct Least Squares Coefficient Adaptation,"*IEEE Transactions on Microwave Theory and Techniques*, vol. 65, no. 3, pp.98–987, 2017.

[18] R. Raich, H. Qian, and G.T. Zhou,"Orthogonal Polynomials for Power Amplifier Modeling and Predistorter Design,"*IEEE Transactions on Vehicular Technology*, vol. 53,no. 5, pp. 1468–1479,Sep. 2004.

[19] R. Raich and G.T. Zhou, "Orthogonal Polynomials for Complex Gaussian Processes". *IEEE Transactions on Signal Processing*, vol. 52, no. 10, pp. 2788–2797, 2004.

[20] O. Hammi, M.Younes and F. M. Ghannouchi,"Metrics and methods for benchmarking of RF transmitter behavioral models with application to the development of a hybrid memory polynomial model," *IEEE Transactions on Broadcasting*, vol. 56, no. 3, pp. 350–357, 2010.

[21] C. Nader, P. Landin, W. Van Moer, et al,"Performance evaluation of peak-to-average power ratio reduction anddigital pre-distortion for OFDM based systems,"*IEEE Transactions on Microwave Theory and Techniques*,vol. 59, no. 12, pp. 3504–3511,2011.